Direct synthesis of multiplexed metal nanowire based devices using carbon nanotubes as vector templates

Article

Accepted Version

Direct synthesis of multiplexed metal nanowire based devices using carbon nanotubes as vector templates

P. Clément, X. Xu, C. T. Stoppiello, G. A. Rance, A. Attanzio, J. N. O'Shea, R. H. Temperton, A. N. Khlobystov, K. R. J. Lovelock, J. M. Seymour, R. M. Fogarty, A. Baker, R. A. Bourne, B. Hall, T. W. Chamberlain* and M. Palma*

We present the synthesis of metal nanowires in a multiplexed device configuration using single-walled carbon nanotubes (SWNTs) as nanoscale vector templates. The SWNT templates control the dimensionality of the wires, allowing precise control of their size, shape and orientation; moreover a solution processable approach enables their linear deposition between specific electrode pairs in electronic devices. Electrical characterizations demonstrate the successful fabrication of metal nanowire electronic devices, while multiscale characterization of the different fabrication steps reveals details of the structure and charge transfer between the material encapsulated and the carbon nanotube. Overall the strategy presented allows facile, low-cost and direct synthesis of multiplexed metal nanowire devices for nanoelectronic applications.

[*] P. Clément [+], X. Xu [+], A. Attanzio, M. Palma*
School of Biological and Chemical Sciences
Materials Research Institute
Queen Mary University of London
London E1 4NS, United Kingdom
E-mail: m.palma@qmul.ac.uk
[+] These authors contributed equally to this work.
C. T. Stoppiello, A. N. Khlobystov
School of Chemistry
University of Nottingham
Nottingham NG7 2RD, United Kingdom
G. A. Rance, A. N. Khlobystov
The Nanoscale and Microscale Research Centre
University of Nottingham
Nottingham NG7 2RD, United Kingdom
J. N. O'Shea, R. H. Temperton
School of Physics
University of Nottingham
Nottingham NG7 2RD, United Kingdom
K. R. J. Lovelock, J. M. Seymour
School of Chemistry, Food and Pharmacy
University of Reading
Reading RG6 6AT, United Kingdom
R. M. Fogarty
Department of Chemistry
Imperial College London
London SW7 2AZ, United Kingdom
A. Baker, R. A. Bourne, B. Hall, T. W. Chamberlain*
Institute of Process Research & Development
School of Chemistry and School of Chemical and Process Engineering
University of Leeds
Leeds LS2 9JT, United Kingdom
E-mail: t.w.chamberlain@leeds.ac.uk
Supporting information for this article is given via

The ability to control the arrangement of materials into highly oriented structures with nanoscale accuracy is of great importance, for a variety of applications including nanoelectronics, energy storage and nanomedicine. Strategies have been proposed, from top-down methods, such as lithography or reactive ion etching,[1] to bottom-up approaches, including wet-chemistry and chemical vapor deposition.[2] While successful, these methodologies suffer from various limitations: top-down strategies are typically costly and time consuming, while the most common bottom-up approaches require high temperatures and employ a metal catalyst, inducing enlarged grain size and contamination, respectively. Notably, these drawbacks have been partially overcome with the use of templates that allow the formation of low-dimensionality nanostructures of a wide range of materials.[3]

In this regard, SWNTs, due to the confinement effects enabled by their nanoscopic tubular design, have been employed as 1D templates to control the position and orientation of molecules or atoms for the construction of nanoscale 1D architectures. Successful examples include the liquid and gas-phase encapsulation of molecules[4] with subsequent nanocrystal growth, and the use of nanotubes as nanoreactors and templates, *via* solution and gas-phase chemical approaches.[5] Additionally, coupling between the material grown and the nanotube was demonstrated, with evidence of electron and/or energy transfer. [6] However, a combination of sonication and density gradient ultracentrifugation is the only approach to have successfully removed newly formed 1D nanostructures from nanotube templates, and most importantly no examples are reported which subsequently use the extracted material for nanoelectronics:[7] it can indeed be desirable to exploit solely metal species in device configurations, for example for sensing applications.

Here we present a strategy for the formation of metal and metal alloy nanowire-based devices employing SWNTs as templates, where a solution processable methodology is employed for the fabrication of distinct (multiplexed) electronic devices on the same chip. Vapors of metal precursors are used to fill the SWNTs that are then dispersed in separate aqueous solutions. Different filled SWNTs are immobilized between

distinct electrode pairs on the same substrate, *via* dielectrophoresis (DEP); thermal annealing is performed to grow the metal/alloy inside the tube. The nanotubes are then removed by oxygen plasma treatment, leaving only the metal nanowires on the substrate, for their electrical characterizations to be performed. This route represents a facile, scalable and environmentally friendly method for the fabrication of arrays of distinct 1D metals in device configurations and on the same chip.

For our studies we employed (7,6) enriched semiconducting SWNTs dispersed in water with sodium dodecyl sulfate (SDS). The nanotubes were initially filled with a Cu containing metal complex precursor, *via* a universal sublimation method as previously reported for $Pt(acac)_2$[2b] and 13 other transition metal complexes.[8] The dimensions of the internal cavity of the SWNTs enables effective encapsulation [see Supporting Information (SI), Figure SI-1]. Copper acetylacetonate ($Cu(acac)_2$) was chosen as a suitable precursor for the Cu system as though it melts at 279-283 °C at ambient pressure,[9] when sealed in a Pyrex ampoule under vacuum, it was found to sublime without decomposition at 110 °C. Thus, heating $Cu(acac)_2$ and SWNTs under vacuum resulted in the gaseous metal complex penetrating the internal channels of the nanotube. After heating, the mixture of SWNTs and complex was rapidly cooled, condensing the complex inside the channels of the SWNT to form $Cu(acac)_2$@SWNT. The SWNTs hybrids were washed several times to remove any excess material from the exterior of the SWNT.[8]

Fluorescence detected X-ray absorption spectroscopy enabled comparison between spectra of the $Cu(acac)_2$@SWNT with free $Cu(acac)_2$ powder and reveals that the shapes of the Cu K edges are very similar after encapsulation. This suggests that the complex remains intact during the filling process and that there is little electronic interaction between the Cu atoms and the nanotube interior (Figures SI-2 and SI-3, and Table SI-1). After decomposition to form Cu@SWNT, the shape of the Cu K edge changes significantly, which is consistent with the reduction of oxidation state of the Cu. Comparison with the edge energies and shapes of Cu foil and Cu(II) complexes, which were used as controls, and time-resolved heating experiments, confirm this change in oxidation state after thermal treatment (see Figures SI-4 and SI-5).

We extended this encapsulation strategy employing $Pt(acac)_2$ and [$Pt(acac)_2$ + $Cu(acac)_2$] precursors with separate SWNT samples; the so formed hybrids after annealing/decomposition will form Pt@SWNT and the alloy Pt-Cu@SWNT, respectively. The location of the metal complex in each sample was confirmed *via* HRTEM and EDX with metal observed solely inside the SWNT in high (>85%) filling yields for all samples (Figure SI-6).[8]

To explore the potential of employing nanotubes as vector templates for the fabrication of metal nanowire devices, the filled SWNTs were immobilized on the same chip between two electrodes in a device configuration, and the effect of the metal (Cu and/or Pt) on the conductivity of the nanotubes was investigated. The use of enriched semiconducting SWNTs for all the device experiments enables the deconvolution of the conductivity of the SWNT and metal complexes and resultant nanowire species.

$Cu(acac)_2$@SWNT, $Pt(acac)_2$@SWNT, and [$Pt(acac)_2$ + $Cu(acac)_2$]@SWNT were dispersed in separate SDS-water solutions and each solution was drop cast on a silicon wafer with pre-patterned electrode pairs (see the SI for full details). The SWNT hybrids were immobilized between the electrode pairs by DEP,[10] in a field effect transistor (FET) configuration, as shown in Figure 1. By repeating this process with different solutions of distinct SWNT hybrids whilst addressing, *via* DEP, different electrode-pair locations on the same substrate surface, it is possible to immobilize distinct metal acetylacetonate ($M(acac)_2$, where M = Cu and/or Pt) SWNT hybrids ($M(acac)_2$@SWNTs) at separate locations on the same chip (see Figure 1 and the SI).[10] Finally, the sample was washed with water to remove the SDS and purged with nitrogen gas.

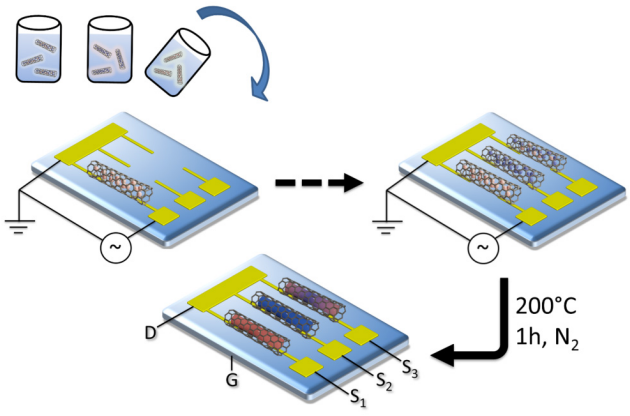

Figure 1: Schematic representation of the deposition of $M(acac)_2$@SWNT by DEP (beige for $Cu(acac)_2$, blue for

$Pt(acac)_2$ and both colors for the Pt-Cu alloy), followed by decomposition of the precursor after annealing. The chip is presented in the FET configuration, where S, D and G are the source, drain and gate electrodes, respectively.

With optimal parameters, a single $M(acac)_2$@SWNT can be immobilized between two electrodes, as demonstrated in the representative Atomic Force Microscopy (AFM) image shown in Figure 2a. Figure 2b-d show representative I_{SD}-V_{SD} curves of the three different $M(acac)_2$@SWNT devices, performed before and after annealing at 200 °C (at which temperature the precursors have been observed to decompose) under N_2 leading to the formation of M@SWNT. We noticed a similar effect on all devices, with a decrease in the measured conductivity upon annealing assigned to changes in the electronic structure of the nanotube, due to the fragmented nature of the guest species not providing a viable conduction pathway. UV-vis and photoluminescence spectroscopy analysis of empty and filled SWNTs (Figures SI-7 and SI-8), reveal shifts and quenching, indicating modification in the electronic states of the filled SWNTs compared to the empty ones. We propose that upon decomposition of the metal precursors (M^{2+}) to form nanowires (M^0) the nature of the guest/nanotube interactions, and consequently the effective density of states of the nanotube, changes resulting in reduction in the conductivity of the nanotubes. [11] A control experiment was performed using pristine empty SWNT in devices before and after annealing; in this case the conductivity was observed to increase after annealing, likely due to the improved electrical contact between the nanotube and the gold electrodes (Figure SI-9a).[12]

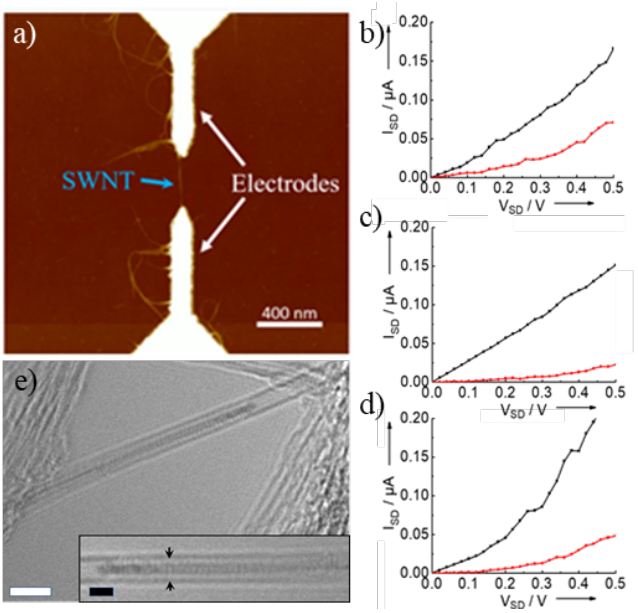

Figure 2: a) AFM topographical image of a single filled SWNT immobilized between two electrodes; I_{SD}-V_{SD} curve characterization of b) $Cu(acac)_2$@SWNT, c) $Pt(acac)_2$@SWNT and d) [$Pt(acac)_2$ + $Cu(acac)_2$]SWNT hybrids after deposition by DEP (black) and after annealing at 200 °C (red). e) HRTEM of a single Cu@SWNT nanotube, black arrows highlight the van der Waals gap between the Cu nanowire and the SWNT: scale bars are 2 nm (white) and 1 nm (black) respectively.

As reported previously,[13] the metal does not grow uniformly inside the nanotubes as there are insufficient metal atoms to form a continuous metal wire inside an individual SWNT (Figure 2e); after annealing at 200 °C we observe the formation of nanoparticles and inhomogeneous nanowires between the electrodes (see Figure SI-10). Therefore, in order to fabricate a homogenous wire, it was necessary to deposit a bundle of $M(acac)_2$@SWNT between the electrodes, instead of an individual filled SWNT; this was done following the same method described previously for a single SWNT but increasing the concentration of the filled SWNT solution and the DEP time. Figure 3a (left) shows a representative AFM image of a small bundle (*ca* 100 nm in height) of $Cu(acac)_2$@SWNT immobilized between an electrode pair. The SWNT shell was then removed by oxygen plasma treatment,[14] while the Cu remained between the two electrodes, exhibiting a height of *ca* 70 nm (Figure 3a right; see also schematic in Figure 3b). It is reasonable to assume that the change in height is due to the removal of the SWNTs. I_{SD}-V_{SD} curves were measured for M@SWNT bundles and we observed a decrease in the conductivity after annealing (Figure 3c); control experiments with a bundle of pristine SWNTs show instead an

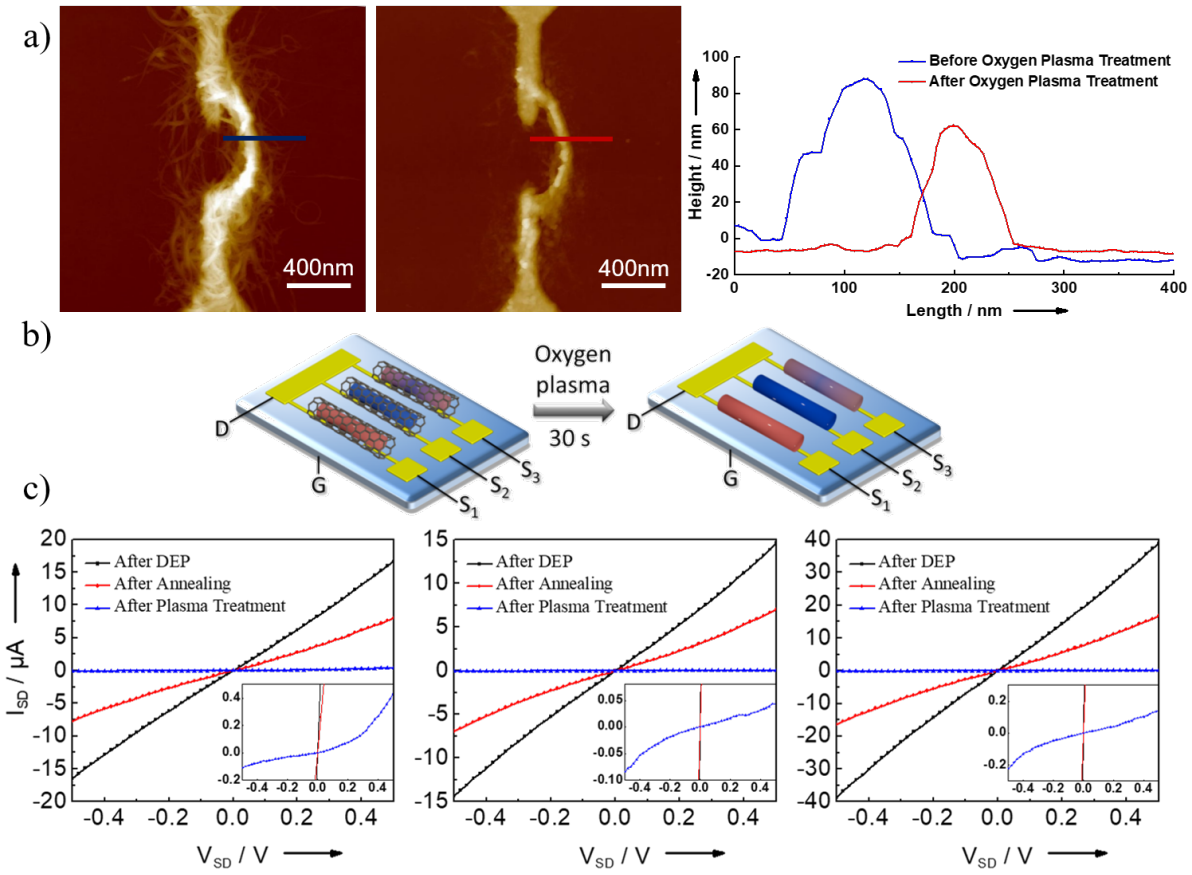

Figure 3: a) AFM topographical images and height profiles of Cu@SWNT before (left) and after (right) oxygen plasma treatment; b) scheme showing the removal of the SWNTs leaving the material grown on the substrate; c) I_{SD}-V_{SD} characterization of bundles of (left to right) $Cu(acac)_2$@SWNT, $Pt(acac)_2$@SWNT and $[Pt(acac)_2 + Cu(acac)_2]$SWNT hybrids after deposition by DEP (black), annealing at 200 °C (red) and plasma treatment (blue).

increase in current after annealing treatment (see Figure SI-9b). Moreover, when the SWNTs were removed *via* oxygen plasma, a sharp decrease in the conductivity was observed, likely due to the lower charge mobility for the pristine metals compared to the M@SWNTs (Figure 3c). The inhomogeneity of the metal wires, the non-optimal contact of these with the macroscopic electrode once the SWNT is removed, and the potential presence of intercalated carbon fragments, might be additional reasons for the observed decrease in conductivity.

To additionally demonstrate the removal of the SWNT shell, gate-dependence measurements were performed. With the presence of the p-type SWNT, the device had a gate dependence for the $M(acac)_2$@SWNT and M@SWNT; nevertheless, this was not observed for Cu, Pt and Pt-Cu nanowires when the SWNTs were removed (see Figure 4, and Figure SI-11). Furthermore, it should be noted that the conductivity measurements of the devices at room temperature indicate that the metals appear to be in their metallic form, even after the short oxygen plasma treatment. This was further verified using a combination of bulk (XPS and Raman spectroscopy) and local probe (TEM and EDX) techniques: see the SI for full details (Figures SI-12-14, and Table SI-2). Additionally, to further understand the electrical properties of these devices, variable-temperature measurements were performed. As shown in Figure SI-15, after plasma treatment, the devices exhibit a temperature dependence in line with previous reports on the electrical properties of metal nanowires.[15]

In summary, we present a solution-processable method of general applicability for the direct synthesis of multiple metal nanowires on the same chip. Different $M(acac)_2$@SWNT were immobilized from solution onto surfaces in nanoscale device configurations, where the SWNTs were used as vector templates. By simple annealing, metal nanowires were grown in the cavity of the nanotubes, which were then removed *via*

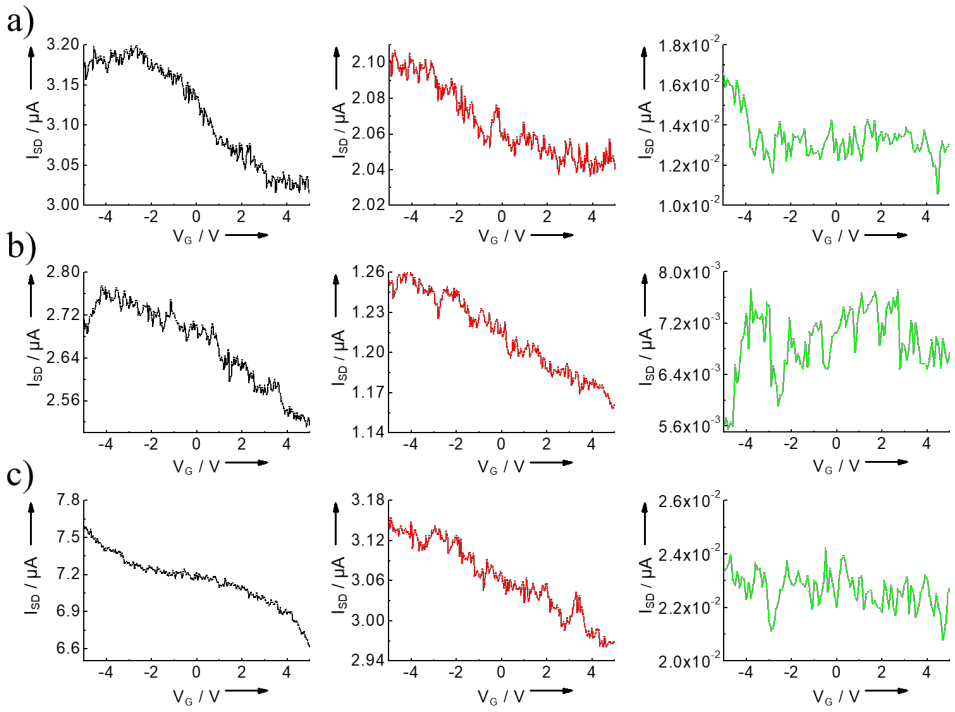

Figure 4: I_{SD}-V_G characterization (V_{SD}=100 mV) with gate dependence of SWNT hybrids after deposition by (left to right): DEP (black), annealing at 200 °C (red) and plasma treatment (green) for: a) $Cu(acac)_2$@SWNT; b) $Pt(acac)_2$@SWNT; and c) Pt-$Cu(acac)_2$@SWNT.

oxygen plasma. Distinct Cu, Pt and Pt-Cu nanowires were successfully synthesized between different electrode pairs on the same chip as indicated by the I-V curves recorded: no gate dependence was observed upon removal of the SWNT shell. This strategy represents a viable route to the large-scale fabrication and detailed exploration of materials properties in controlled 1D architectures. The universal nature of the SWNT filling method allows a broad range of individual metals and an almost infinite number of metal combinations in alloy form to be incorporated; this in turn means that our approach has the potential to impact upon a broad range of fields, from nanoelectronics applications with low power consumption such as chemical sensors or quantum information processing, to lab-on-a-chip based tunable electrocatalytic arrays.

ACKNOWLEDGMENTS

T.W.C would like to acknowledge the UK CatalysisHub, University of Leeds, B18 and I20 (Diamond, experiments SP20523 and SP21167) and BM25 (ESRF, experiment CH-4680). C.T.S., G.A.R., and A.N.K. acknowledge the Nanoscale & Microscale Research Centre for access to instrumentation. M.P., R.A.B and T.W.C. gratefully acknowledge the Engineering and Physical Science Research Council under awards EP/M029506/1, EP/L015285/1 and EP/K014714/1. X.X is financially supported by the China Scholarship Council.

Keywords: nanotubes; template synthesis; nanostructures; nanotechnology

REFERENCES:

[1] a) L. Lee, B. Kang, S. Han, H. eun Kim, M. D. Lee, J. H. Bang, *Small* **2018**, *14*, 1–8. b) V. Mondiali, M. Lodari, M. Borriello, D. Chrastina, M. Bollani, *Microelectron. Eng.* **2016**, *153*, 88–91. c) W. Chen, D. Deng, *Chem. Commun.* **2014**, *50*, 13327–13330. d) G. Anoop, T. Y. Kim, H. J. Lee, V. Panwar, J. H. Kwak, Y. J. Heo, J. H. Yang, J. H. Lee, J. Y. Jo, *Adv. Electron. Mater.* **2017**, *3*, 1–11.

[2] a) H. Xu, Z. Ding, C. T. Nai, Y. Bao, F. Cheng, S. J. R. Tan, K. P. Loh, *Adv. Funct. Mater.* **2017**, 27, 1603887. b) R. M. Jacobberger, M. S. Arnold, *ACS Nano* **2017**, 11, 8924–8929. c) A. Attanzio, A. Sapelkin, F. Gesuele, A. van der Zande, W. P. Gillin, M. Zheng, M. Palma, *Small* **2017**, 13, 1–5. d) M. Freeley, A. Attanzio, A. Cecconello, G. Amoroso, P. Clement, G. Fernandez, F. Gesuele, M. Palma, *Adv. Sci.* **2018**, 5, 1800596.

[3] a) A. Rao, H. Long, A. Harley-Trochimczyk, T. Pham, A. Zettl, C. Carraro, R. Maboudian, *ACS Appl. Mater. Interfaces* **2017**, 9, 2634–2641. b) J. M. Song, J. S. Lee, *Sci. Rep.* **2016**, 6, 1–7. c) T. Bayrak, S. Helmi, J. Ye, D. Kauert, J. Kelling, T. Schönherr, R. Weichelt, A. Erbe, R. Seidel, *Nano Lett.* **2018**, 18, 2116–2123. d) S. Sandoval, D. Kepić, Á. Pérez Del Pino, E. György, A. Gómez, M. Pfannmoeller, G. Van Tendeloo, B. Ballesteros, G. Tobias, *ACS Nano* **2018**, 12, 6648–6656.

[4] a) S. Cambré, W. Wenseleers, E. Goovaerts, *J. Phys. Chem. C* **2009**, 113, 13505–13514. b) T. W. Chamberlain, J. Biskupek, G. A. Rance, A. Chuvilin, T. J. Alexander, E. Bichoutskaia, U. Kaiser, A. N. Khlobystov, *ACS Nano* **2012**, 6, 3943–3953. c) S. Cambré, W. Wenseleers, *Angew. Chemie - Int. Ed.* **2011**, 50, 2764–2768. d) L. Shi, P. Rohringer, M. Wanko, A. Rubio, S. Waßerroth, S. Reich, S. Cambré, W. Wenseleers, P. Ayala, T. Pichler, *Phys. Rev. Mater.* **2017**, 075601, 1–7. e) X. Ma, S. Cambré, W. Wenseleers, S. K.

Doorn, H. Htoon, *Phys. Rev. Lett.* **2017**, 118, 1–7.

[5] a) J. Zhang, D. Zhao, D. Xiao, C. Ma, H. Du, X. Li, L. Zhang, J. Huang, H. Huang, C. L. Jia, et al., *Angew. Chemie - Int. Ed.* **2017**, 56, 1850–1854. b) C. T. Stoppiello, J. Biskupek, Z. Y. Li, G. A. Rance, A. Botos, R. M. Fogarty, R. A. Bourne, J. Yuan, K. R. J. Lovelock, P. Thompson, et al., *Nanoscale* **2017**, 9, 14385–14394. c) P. V. C. Medeiros, S. Marks, J. M. Wynn, A. Vasylenko, Q. M. Ramasse, D. Quigley, J. Sloan, A. J. Morris, *ACS Nano* **2017**, 11, 6178–6185. d) M. V. Kharlamova, J. J. Niu, *Appl. Phys. A Mater. Sci. Process.* **2012**, 109, 25–29. e) T. Cui, X. Pan, J. Dong, S. Miao, D. Miao, X. Bao, *Nano Res.* **2018**, 11, 3132–3144. f) R. Carter, L. Oakes, N. Muralidharan, A. P. Cohn, A. Douglas, C. L. Pint, *ACS Appl. Mater. Interfaces* **2017**, 9, 7185–7192. g) S. Sandoval, E. Pach, B. Ballesteros, G. Tobias, *Carbon N. Y.* **2017**, 123, 129–134. h) Z. Aslam, J. G. Lozano, R. J. Nicholls, A. A. Koos, F. Dillon, M. C. Sarahan, P. D. Nellist, N. Grobert, *J. Alloys Compd.* **2017**, 721, 501–505. i) L. Shi, K. Yanagi, K. Cao, U. Kaiser, P. Ayala, T. Pichler, *ACS Nano* **2018**, 12, 8477–8484.

[6] a) R. Marega, D. Bonifazi, *New J. Chem.* **2014**, 38, 22–27. b) M. Martincic, G. Tobias, *Expert Opin. Drug Deliv.* **2015**, 12, 563–581. c) K. Ramachandran, T. Raj Kumar, K. J. Babu, G. Gnana Kumar, *Sci. Rep.* **2016**, 6, 1–12. d) S. Brahim, S. Colbern, R. Gump, A. Moser, L. Grigorian, *Nanotechnology* **2009**, 20, 235502. e) M. V. Kharlamova, C. Kramberger, O. Domanov, A. Mittelberger, K. Yanagi, T. Pichler, D. Eder, *J. Mater. Sci.* **2018**, 53, 13018–13029. f) G. Tobias, B. Ballesteros, M. L. H. Green, *Phys. Status Solidi Curr. Top. Solid State Phys.* **2010**, 7, 2739–2742. g) C. Spinato, A. Perez Ruiz De Garibay, M. Kierkowicz, E. Pach, M. Martincic, R. Klippstein, M. Bourgognon, J. T. W. Wang, C. Ménard-Moyon, K. T. Al-Jamal, et al., *Nanoscale* **2016**, 8, 12626–12638. h) S. Van Bezouw, D. H. Arias, R. Ihly, S. Cambré, A. J. Ferguson, J. Campo, J. C. Johnson, J. Defillet, W. Wenseleers, J. L. Blackburn, *ACS Nano* **2018**, 12, 6881–6894.

[7] a) J. Zhang, Y. Miyata, R. Kitaura and H. Shinohara, *Nanoscale* **2011**, 3, 4190-4194. b) J. Zhang, F. Zhou, Y. Miyata, R. Kitaura, H. Su and H. Shinohara, *RSC Advances* **2013**, 3. c) L. Shi, K. Yanagi, K. Cao, U. Kaiser, P. Ayala and T. Pichler, *ACS Nano* **2018**, 12, 8477–8484.

[8] a) K. Cao, T. Zoberbier, J. Biskupek, A. Botos, R. L. McSweeney, A. Kurtoglu, C. T. Stoppiello, A. V. Markevich, E. Besley, T. W. Chamberlain, et al., *Nat. Commun.* **2018**, 9, 1–10. b) A. Botos, J. Biskupek, T. W. Chamberlain, G. A. Rance, C. T. Stoppiello, J. Sloan, Z. Liu, K. Suenaga, U. Kaiser, A. N. Khlobystov, *J. Am. Chem. Soc.* **2016**, 138, 8175–8183. c) T. Zoberbier, T. W. Chamberlain, J. Biskupek, N. Kuganathan, S. Eyhusen, E. Bichoutskaia, U. Kaiser, A. N. Khlobystov, *J. Am. Chem. Soc.* **2012**, 134, 3073–3079.

[9] M. V. Buzaeva, V. V. Dubrovina, O. A. Davydova, E. S. Klimov, *Russ. J. Appl. Chem.* **2011**, 84, 892–894.

[10] X. Xu, P. Clément, J. Eklöf-Österberg, N. Kelley-Loughnane, K. Moth-Poulsen, J. L. Chávez, M. Palma, *Nano Lett.* **2018**, 18, 4130–4135.

[11] R. L. McSweeney, T. W. Chamberlain, M. Baldoni, M. A. Lebedeva, E. S. Davies, E. Besley, A. N. Khlobystov, *Chem. Eur J.* **2016**, 22(38), 13540-13549.

[12] J. Lee, C. Park, J. Kim, J. Kim, *J. Phys. D: Appl. Phys.* **2000**, 33, 1953–1956.

[13] T. W. Chamberlain, T. Zoberbier, J. Biskupek, A. Botos, U. Kaiser, A. N. Khlobystov, *Chem. Sci.* **2012**, 3, 1919–1924.

[14] X. Guo, J. P. Small, J. E. Klare, Y. Wang, M. S. Purewal, I. W. Tam, B. H. Hong, R. Caldwell, L. Huang, S. O. Brien, et al., *Science* **2011**, 356, 356–360.

[15] R. Venkatesh, S. Kundu, A. Pradhan, T. P. Sai, A. Ghosh, N. Ravishankar, *Langmuir* **2015**, *31*, 9246–9252.

Table of Contents Graphic

Metal and metal alloy nanowires were formed employing carbon nanotubes as nanoscale vector templates; a solution processable methodology allowed for the fabrication of multiplexed electronic devices on the same chip.